Electronic Supplementary Material (ESI) for New Journal of Chemistry.
This journal is © The Royal Society of Chemistry and the Centre National de la Recherche Scientifique 2016

Electronic Supporting Information

Support Effects in Rare Earth Element Separation Using Diglycolamide-Functionalized Mesoporous Silica

Estelle Juère[a,b], Justyna Florek[a,b], Dominic Larivière[a,c]*, Kyoungsoo Kim[d] and Freddy Kleitz[a,b]*

[a]Department of Chemistry, Université Laval, Québec, Canada G1V 0A6. E-mail: freddy.kleitz@chm.ulaval.ca; dominic.lariviere@chm.ulaval.ca; Fax: +1-418-656-7916; Tel: +1-418-656-7812.
[b]Centre de Recherche sur les Matériaux Avancés (CERMA), Université Laval, Québec, Canada G1V 0A6.
[c]Centre en Catalyse et Chimie Verte (C3V), Université Laval, Québec, Canada G1V 0A6.
[d]Center for Nanomaterials and Chemical Reactions, Institute for Basic Science (IBS), Daejeon 305-701, Korea.

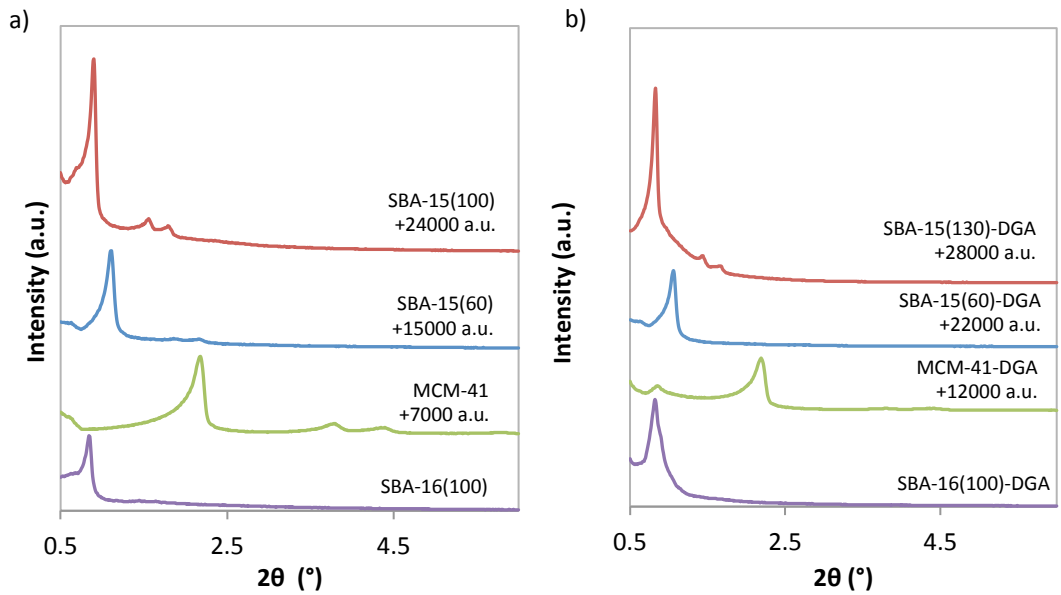

Figure S1: Low angle powder XRD patterns of a) the pure; b) the functionalized materials.

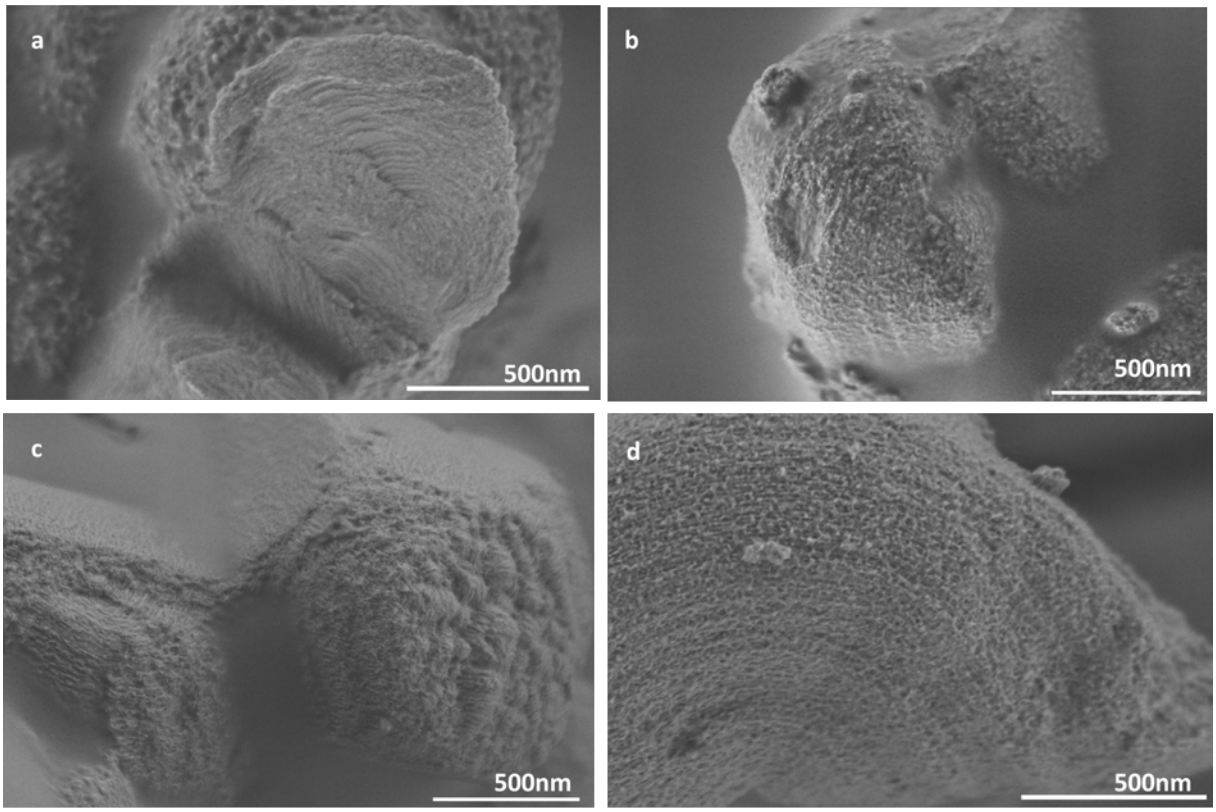

Figure S2: Representative HRSEM images of MCM-41-DGA (a), SBA-15(60)-DGA (b) and SBA-15(100)-DGA (c, d).

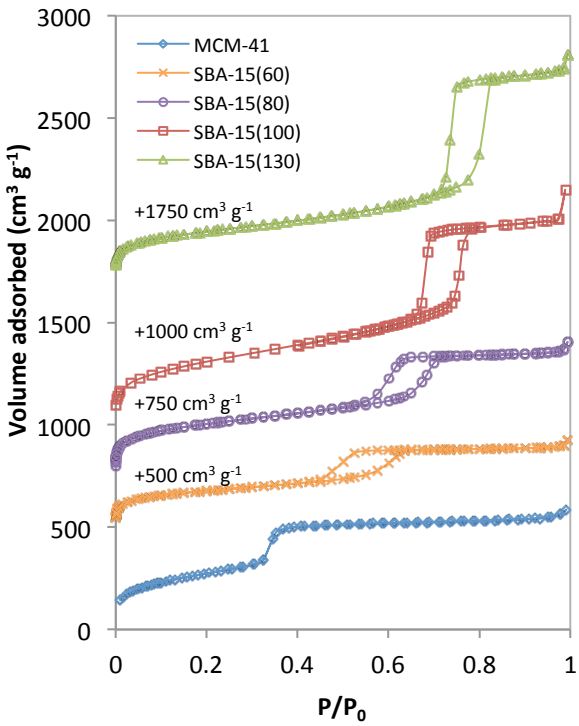

Figure S3: N_2 sorption isotherms (-196°C) of the pure SBA-15 materials aged at different temperatures and MCM-41, as indicated.

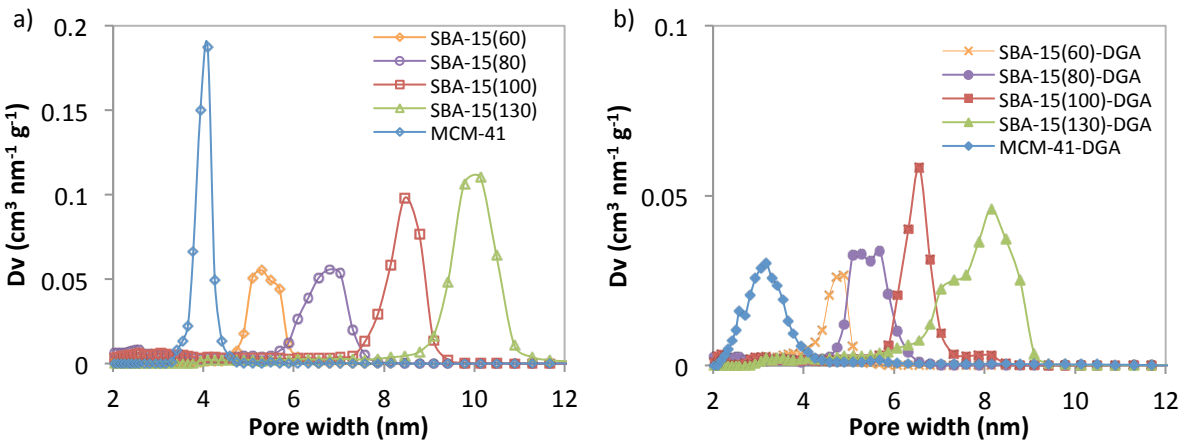

Figure S4: NLDFT pore size distributions calculated from the desorption branch for cylindrical pore model of a) the pure SBA-15 and MCM-41 materials b) the corresponding grafted silica materials.

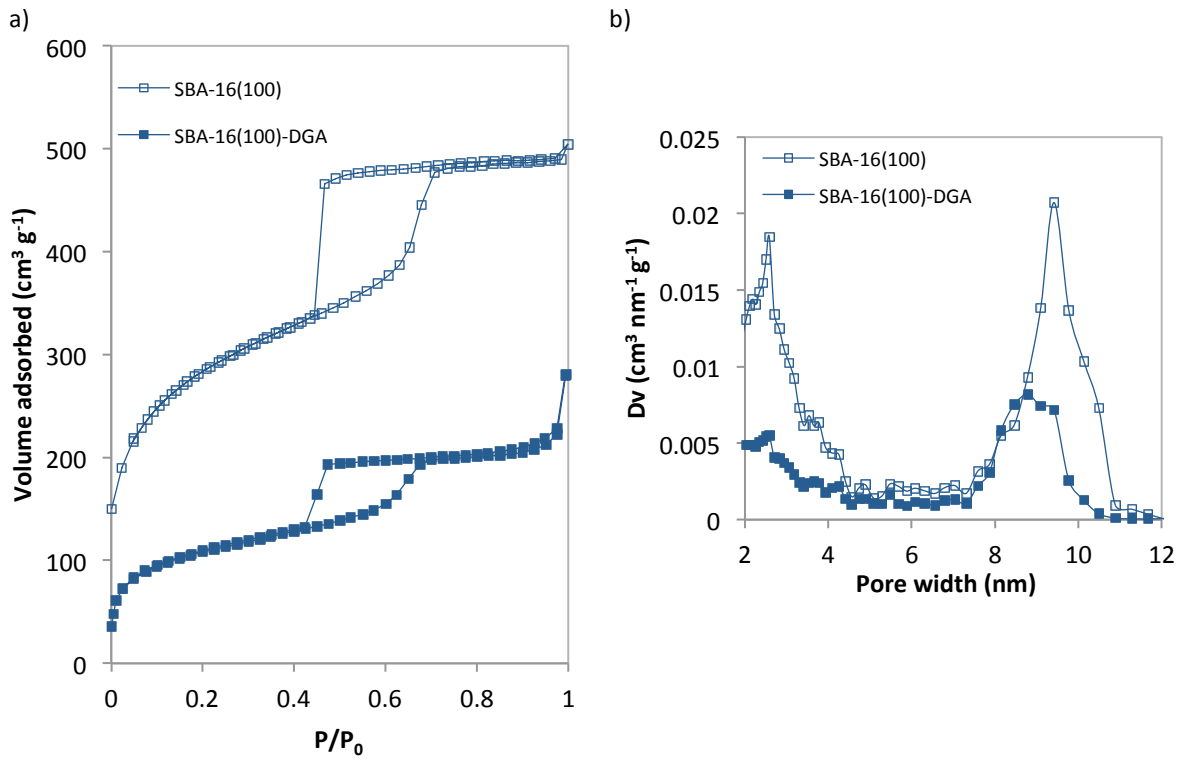

Figure S5: a) N_2 physisorption isotherms of pure SBA-16 and the corresponding grafted SBA-16-DGA measured at -196°C. b) NLDFT pore size distributions of SBA-16 and SBA-16-DGA calculated from the adsorption branch for spherical pore model.

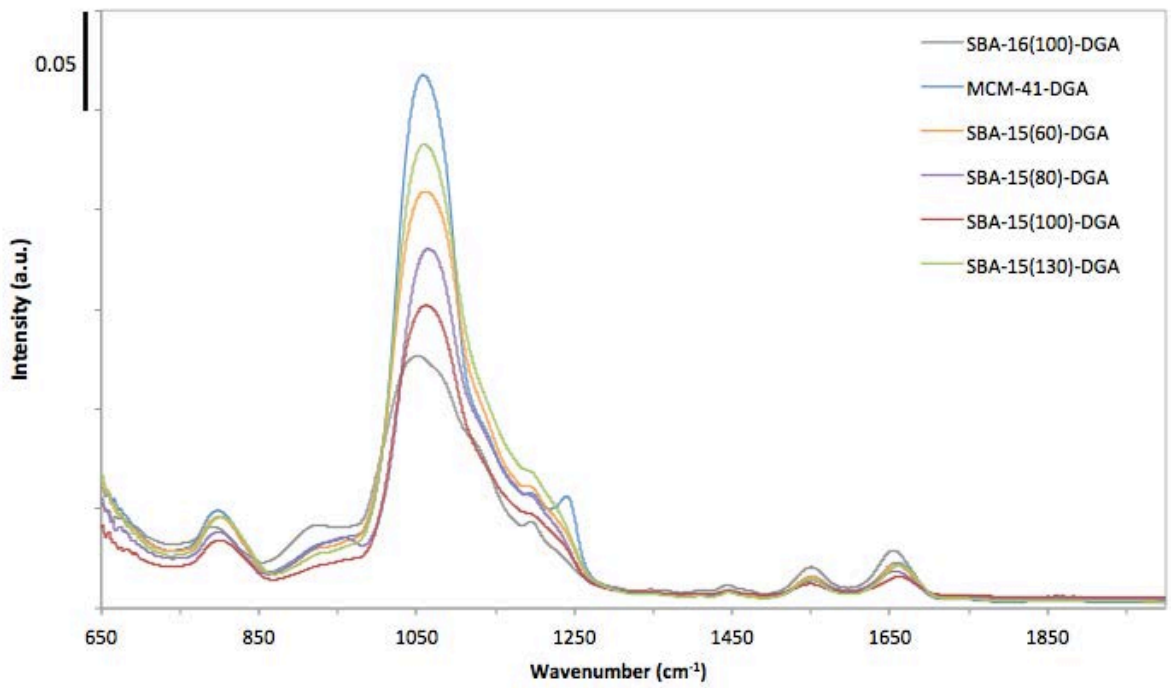

Figure S6: IR spectra of all the DGA-functionalized samples.

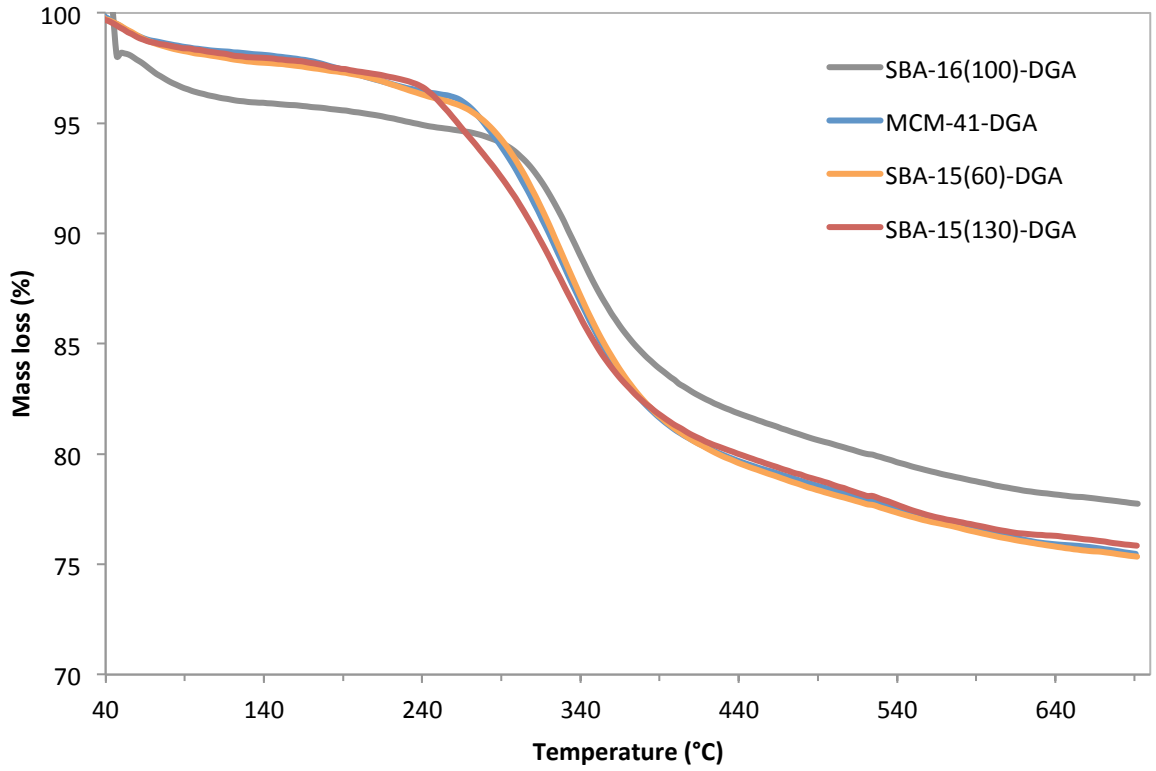

Figure S7: Mass loss profiles obtained from the TGA analysis with the air flow 40 mL min^{-1} for the representative DGA functionalized silica materials.

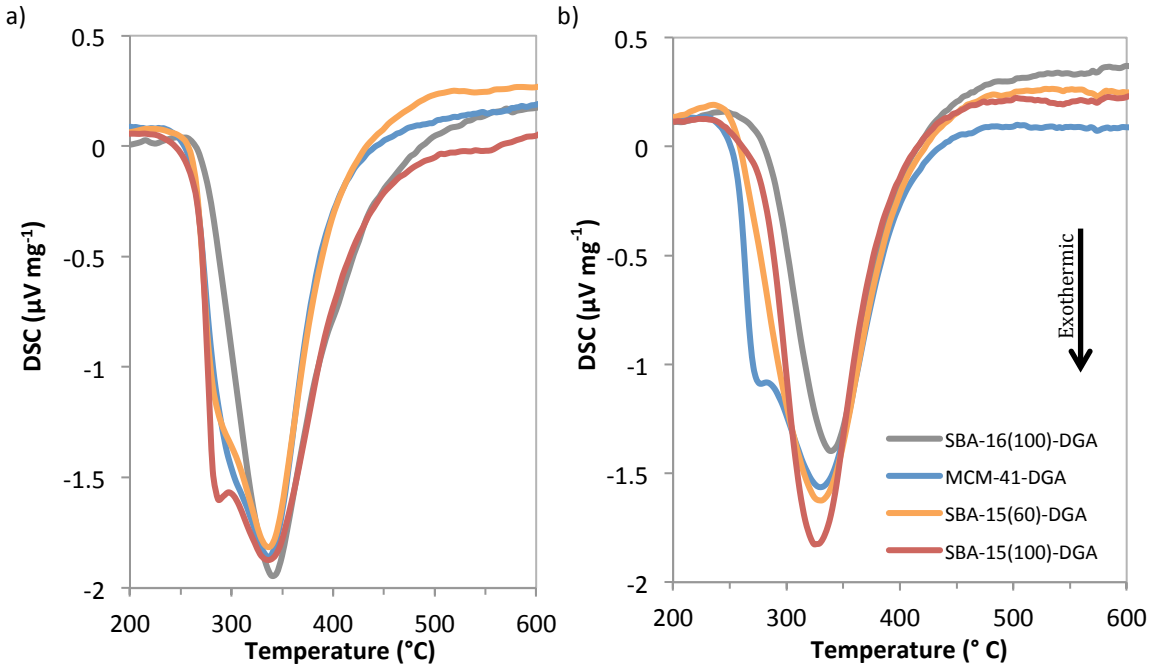

Figure S8: DSC profile of the samples SBA-16(100)-DGA, MCM-41-DGA, SBA-15(60)-DGA and SBA-15(100)-DGA obtained with a) air flow of 20 mL min^{-1} and b) air flow of 40 mL min^{-1}.

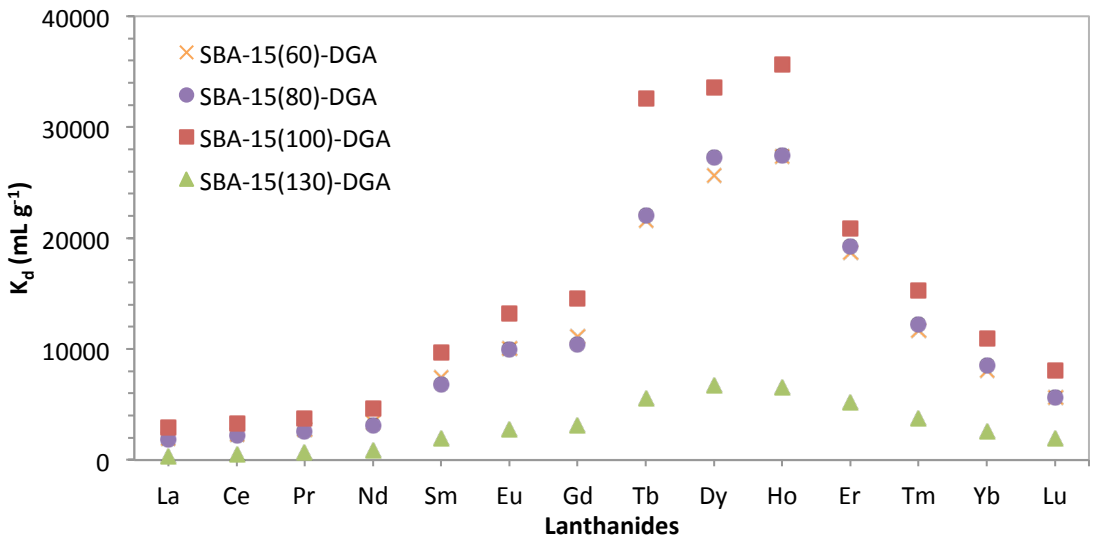

Figure S9: Ln extraction (K_d) of the DGA grafted SBA-15 materials with various pore sizes.

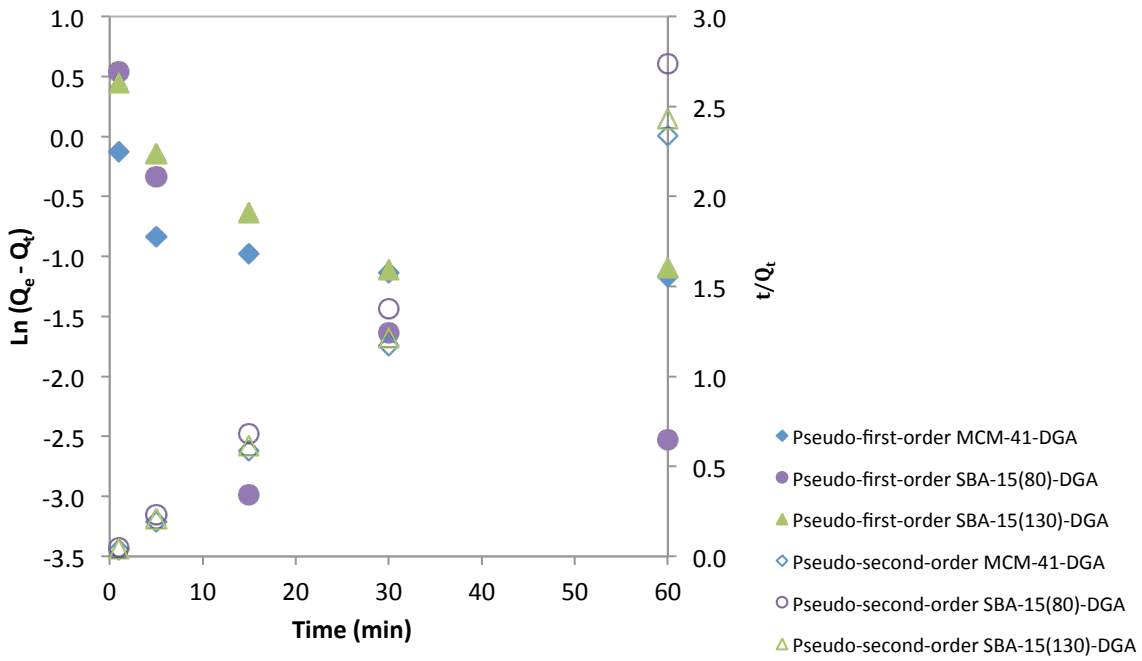

Figure S10: Linear regression of the pseudo-first- order and the pseudo-second-order of SBA-15(80)-DGA, SBA-15(130)-DGA and MCM-41-DGA.

$Q_t = Q_e(1 - e^{-k_1 t})$: Pseudo-first-order equation where Q_t (µg g^{-1}) and Q_e (µg g^{-1}) represent the amount of REEs captured at time t and at equilibrium, respectively and k_1 represents the rate constant (L min^{-1});

$Q_t = \frac{k_2 Q_e^2 t}{1+k_2 Q_e t}$: Pseudo-second-order equation where Q_t (µg g^{-1}) and Q_e (µg g^{-1}) represent the amount of REEs captured at time t and at equilibrium, respectively and k_2 represents the rate constant (L min^{-1}).

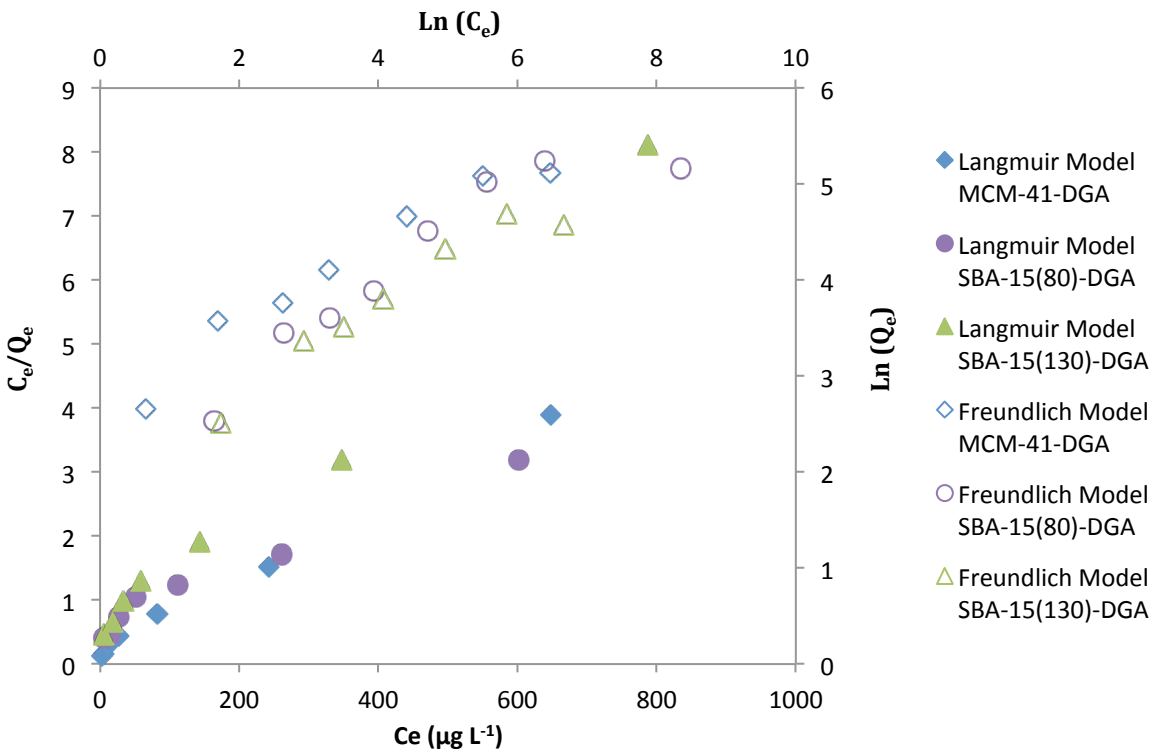

Figure S11: Linear regression of the Langmuir and the Freundlich models used for the adsorption isotherms experiments

$Q_e = Q_{max}\left(\frac{K_L C_e}{1+K_L C_e}\right)$: Langmuir equation where Q_{max} (µg g^{-1}) is the maximum capacity of the materials, K_L (L µg^{-1}) is the Langmuir affinity constant;

$Q_e = K_F {C_e}^{1/n}$: Freundlich equation where K_F (µg g^{-1}) is the Freundlich adsorption capacity constant and 1/n refers to favorable adsorption if comprised in the interval $0 < 1/n < 1$.

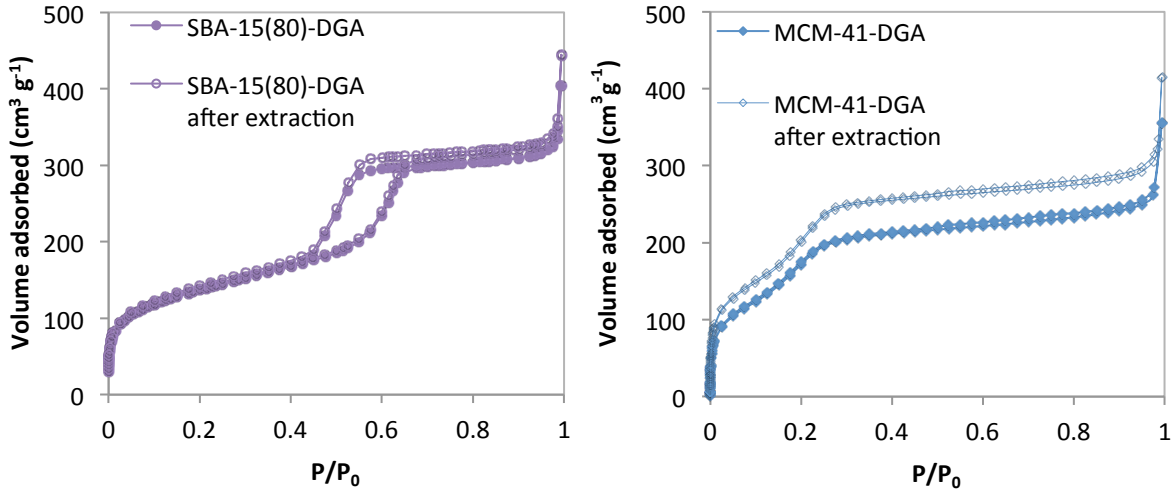

Figure S12: N_2 sorption isotherms (-196°C) of SBA-15(80)-DGA and MCM-41-DGA before and after being used 4 times.

Table S1: CHN analysis of the grafted samples.

Sample	Carbon (%)	Hydrogen (%)	Nitrogen (%)
SBA-16-DGA	9.32	2.53	2.03
SBA-15(60)-DGA	12.17	2.14	2.68
SBA-15(80)-DGA	12.08	2.48	2.58
SBA-15(100)-DGA	11.68	2.25	2.50
SBA-15(130)-DGA	11.36	2.02	2.55
MCM-41-DGA	12.40	2.36	2.74

Table S2: Parameters derived from the pseudo-first-order, pseudo-second-order, Langmuir and Freundlich models.

		SBA-15(80)-DGA	SBA-15(130)-DGA	MCM-41-DGA
Pseudo-first-order	$Q_{e,th}$	0.61	1,00	0.56
	k_1	0.040	0.023	0.013
	r^2	0.4293	0.6805	0.5066
Pseudo-second-order	$Q_{e,th}$	21.95	24.70	25.70
	k_2	0.45	0.43	1.29
	r^2	0.9999	0.9999	1
Langmuir model	Q_m	261.8	106.5	176.2
	K_L	0.0058	0.018	0.027
	r^2	0.9901	0.9888	0.9964
Freundlich model	K_F	6.68	7.13	14.25
	1/n	0.52	0.44	0.42
	r^2	0.9708	0.9389	0.9519